Wrench Estimation of Modular Manipulator with External Actuation and Joint Locking

Yonghyeok Kim, Hasun Lee, Jeongseob Lee and Dongjun Lee

***Abstract*— This paper proposes an external wrench estimation method for modular manipulators, where each link module is driven with external actuation (e.g., rotors, thrusters) and inter-module joints can be locked to increase end-effector stiffness or workforce of the manipulator. For such systems, the commonly-used momentum-based observer (MBO [1]) is not suitable due to the presence of unknown joint locking (JL) torque and also the degeneracy of Jacobian transpose relation with the system degree-of-freedom (DOF) becoming less than six with the joint locking. To overcome this, we propose two novel external wrench estimation algorithms: a distributed algorithm based on recursive Newton-Euler dynamics and a centralized algorithm based on D'Alembert's principle, both using an F/T (force/torque) sensor at the base. Experiments are conducted to demonstrate the effectiveness of the proposed algorithms.**

I. Introduction

Traditional robot manipulators utilize internal actuation, where the actuators produce force or torque at the joints between consecutive links (Fig. 1a). In other words, the actuators produce force or torque at the joint associated with the relative motion between two consecutive links. In contrast, a new class of manipulators has recently been proposed, known as externally-actuated modular manipulator (EAMM) ([2], [3], [4], [7], [14]). In this type of manipulator, each link is driven by external actuation, such as rotors or thrusters, which means that the control actuation is associated with the absolute link twist instead of the relative inter-link motion, as is the case with internal actuation (Fig. 1b).

This EAMM, with each actuator compensating for its own link weight has the potential to realize a lightweight, long, and slender manipulator with scalable characteristics. This enables operation within a narrow and deep workspace (e.g., 5∼10m), which is not achievable with internally-actuated manipulators. Internally-actuated manipulators tend to be excessively bulky and heavy to achieve similar tasks.

Utilizing the scalability of EAMM for aerial manipulation in an extended workspace is a significant advantage, as it is challenging to achieve with typical drone-based aerial platforms (e.g., [5], [10], [12], [11]), which often face limitations such as short operation time, limited payload, and difficulties in control and sensing during flight. However, despite these advantages, EAMM's end-effector workforce (or stiffness) mainly relies on the capacity of the distal link, potentially leading to insufficiency for certain applications.

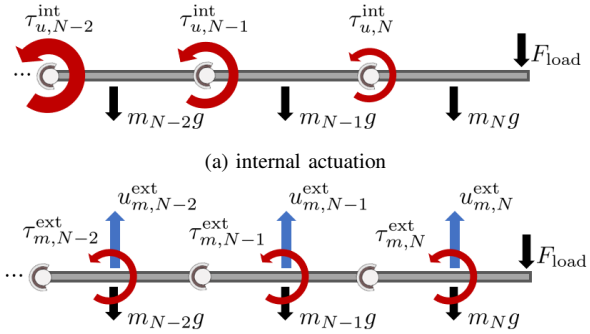

(a) internal actuation

(b) external actuation

Fig. 1: Illustration of types of robot manipulator actuation: (1a) internal actuation and (1b) external actuation.

To increase the end-effector workforce in EAMM, the idea of joint locking (JL) has been proposed (i.e., EAMM-JL, [2], [3]), which essentially make a group of distal joints locked with each other so that they, collectively, behave as one single large link, thereby, significantly increasing the end-effector workforce. In this paper, we consider the problem of end-effector external wrench estimation of this class of EAMM-JL. We particularly focus on our recently-proposed EAMM-JL system LASDRA (large-size aerial skeleton with distributed rotor actuation, [2]), the obtained results are applicable to other kinds of EAMM-JL.

End-effector external wrench information is useful for various manipulator control methods by compensating this wrench or monitoring the workspace wrench. Of course, the easiest way to obtain this external wrench information is to deploy an F/T sensor at the end-effector. This, however, turns out not so suitable for EAMM-JL (e.g., for LASDRA [2], [3]), as commercially-available F/T sensors are too heavy to accommodate (e.g., ATI$^{\text{TM}}$ F/T sensor with control box of around 1.1kg) or has too small range of sensing (e.g., AIDIN$^{\text{TM}}$ Miniature F/T sensor only 3.2g, yet, sensing range less than 25N/0.15Nm).

Another popular method for external wrench estimation is to utilize momentum-based observer (MBO) [1], [6], [7]. This standard MBO, however, is not so suitable either for EAMM-JL, particularly when many joints are locked, since: 1) the joint locking torque is often not known (e.g., due to not-backdrivable/high-friction transmission), which the

This work was supported by the National Research Foundation of Korea (NRF) grant funded by the Korea government (MSIT) (No. NRF-2020R1A2C3010039).

Y. Kim, J. Lee, and D. J. Lee are with the Department of Mechanical Engineering, IAMD and IOER, Seoul National University, Seoul 08826, Republic of Korea. {yhkim83, overjs94, djlee}@snu.ac.kr. Corresponding author: Dongjun Lee

H. Lee was with the Department of Mechanical Engineering, Seoul National University and is currently with Stradvision, Seoul 06621, Republic of Korea. hasun.lee@stradvision.com.

MBO cannot distinguish from the external wrench torque; and 2) if so many joints are locked that the remaining system degree-of-freedom (DOF) becomes less than six, the manipulator Jacobian mapping relation between the external wrench (in se(3)) and its reflected joint torque becomes degenerate and we cannot recover the full six-dimensional external wrench information from the MBO with dimension less than six. Note that the ability to estimate a full six-dimensional external wrench can still be important even with excessive joint locking (e.g., releasing some locked joints for compliant interaction and safety if pushed/jammed by environments/obstacles).

To address these issues, in this paper, we propose two new external wrench estimation algorithms for EAMM-JL: 1) a distributed algorithm based on the recursive Newton-Euler dynamics; and 2) a centralized algorithm based on D'Alembert's principle. To overcome the aforementioned issues of Jacobian-degeneracy and uncertain JL-torques, both algorithms require an F/T sensor at the base, which is accommodatable by EAMM-JL (i.e., heavy sensors can be attached at the base). The distributed algorithm estimates the end-effector wrench by estimating internal joint wrenches between the links sequentially from the base. Here, MBO in maximal coordinates for each link to calculate internal joint wrenches using the recursive Newton-Euler dynamics. This distributed algorithm is particularly suitable for EAMM-JL, as its algorithm and the required communication are all modular. The performance of this distributed algorithm, however, can degrade through the inter-link prorogation, particularly if the number of links becomes large with a certain set of gains, similar to the issue of string stability [15]. On the other hand, our centralized algorithm is free from this issue, i.e., from being based on the D'Alembert's principle, it estimates the external force applied to the entire system at once, eliminating the effect of the inter-link propagation error while also providing a precise external wrench estimation even if the system DOF is reduced less than six through joint locking and the end-effector Jacobian becomes singular.

The rest of this paper is organized as follows: Sec. II provides a preliminary explanation of the LASDRA system with joint locking and the MBO. Sec. III describes the distributed wrench estimation algorithm, and Sec. IV presents the D'Alembert's principle-based wrench estimation. Sec. V presents simulation and experimental results to validate the proposed algorithms. Sec. VI contains some concluding remarks along with future research directions.

II. Preliminary

A. LASDRA system with joint locking

The large-size aerial skeleton system with distributed rotor actuation (LASDRA) [2] is a lightweight, EAMM-JL aerial robot arm platform designed for aerial manipulation. LASDRA utilizes rotor-based actuation through omni-directional aerial robots (ODAR) [5] to achieve a significant work force and manipulate large form factors. Unlike internal actuation methods such as electric motors and hydraulic drivers,

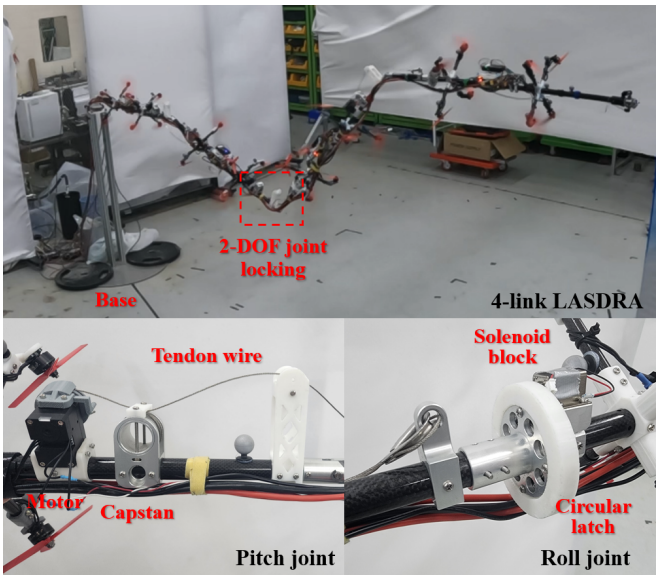

Fig. 2: A 4-link LASDRA flight with joint locking device: Capstan brake mechanism for pitch joint and latch mechanism for roll joint.

LASDRA's distributed external actuation system allows producing significant work force and estimating precise pose estimation [4]. Each ODAR generates its own body wrench $(u^b_{m,i}, \tau^b_{m,i}) \in \mathbb{R}^6$ through a mapping matrix $B \in \mathbb{R}^{6\times 8}$ from a thrust vector $\lambda_i \in \mathbb{R}^8$, as described by

$$\begin{pmatrix} u^b_{m,i} \\ \tau^b_{m,i} \end{pmatrix} = B\lambda_i \tag{1}$$

where i represents the index of the link and $\star^b$ denotes that $\star$ is expressed in its body frame. The wrench generated by each ODAR enables external actuation of the LASDRA system. This external actuation like Fig.(1b) can make the system scalable and gravity-defying [3]. In addition, with this external actuation, the base experience less load as compared to the case of internal actuation, allowing us to install an F/T sensor at the base with a reasonable sensing range. An essential aspect of LASDRA is its joint locking mechanism, which employs a mechanical element to lock the joints, thereby enabling the generation of significant payload forces. To distribute the external payload of the distal link across the other links and generate a larger wrench at the end-effector, a joint locking device is installed on each link of the LASDRA platform. Fig. 2 shows 2-DOF joint locking devices used in LASDRA, with a Capstan brake used in the pitch-direction joint and a latch mechanism used in the roll-direction joint.

B. Momentum based observer

The momentum-based observer (MBO) [1] is a widely used method for estimating external wrench acting on a robotic manipulator by analyzing changes in momentum. The robot system is modeled by

$$\mathbf{M}(q)\ddot{q} + \mathbf{C}(q,\dot{q})\dot{q} + \mathbf{g}(q) = \tau_u + \tau_l + \tau_{ext} \tag{2}$$

where $n \in \mathbb{N}$ is degree of freedom, $\mathbf{M}(q) \in \mathbb{R}^{n\times n}$ represents the inertia matrix, $\mathbf{C}(q,\dot{q}) \in \mathbb{R}^{n\times n}$ represents the Coriolis

matrix, $\mathbf{g}(q) \in \mathbb{R}^n$ represents the gravity matrix, and $q \in \mathbb{R}^n$ represents the joint angle. The input torque generated by manipulator, joint locking torque due to joint locking devices, and torques generated by an external wrench are represented by $\tau_u, \tau_l, \tau_{ext} \in \mathbb{R}^n$ respectively. Unlike other methods, MBO does not require the use of acceleration information and the inversion of the inertia matrix. MBO is defined by recursive integration of change of momentum and additional integrand terms to make observer output r, the so-called, residual vector, converge to the external joint torque τ_{ext} in the first-order differential equation. The formula for standard MBO in generalized coordinates is described by

$$\begin{aligned} \beta(q,\dot{q}) &:= \mathbf{g}(q) - \mathbf{C}^T(q,\dot{q})\dot{q} \\ r(t) &:= K_O[p(t) - \int_0^t (\tau_u + \tau_l - \beta + r)\, ds - p(0)] \\ K_O &= \text{diag}[k_{O,i}] \end{aligned} \tag{3}$$

where, $p := \mathbf{M}\dot{q} \in \mathbb{R}^n$ is the generalized momentum, and $K_O \in \mathbb{R}^{n\times n}$ is the observer gain of each joint. The input joint torque of LASDRA can then be computed by

$$\tau_u = \sum_{i=1}^{N} \tau_{u,i} = \sum_{i=1}^{N} J_{ci}^T \begin{pmatrix} u_{m,i} \\ \tau_{m,i} \end{pmatrix} \tag{4}$$

where N denotes the number of ODAR links and $\tau_{u,i} \in \mathbb{R}^n$ represents the joint torque generated by i-th ODAR and $J_{ci} \in \mathbb{R}^{6\times n}$ is the Jacobian matrix that maps the joint velocity to the twist of the i-th ODAR link.

However, when joint locking is used to generate locking torque, it becomes impossible to use standard MBO since the locking torque τ_l and the external joint torque from the end-effector τ_{ext} become indistinguishable. Although it is possible to apply standard MBO by calculating the adjacent locked links as a lumped mass, this calculation becomes complicated. Furthermore, if the degree of freedom decreases due to joint locking and becomes less than 6, the observer cannot estimate 6-DOF external wrench information. This is because to estimate the end-effector's external wrench, a proper mapping between the estimated (unlocked) external joint torque to the 6-DOF information of the external wrench (3-axis force and 3-axis torque) is required. Thus, if joints are locked, and the remaining degree of freedom is less than 6, MBO is not applicable to estimate the external wrench at the end-effector. [1] In terms of mathematical representation, the mapping matrix from the external joint torque to the external wrench at the end-effector is denoted by $(J_{EF}^T)^\dagger$. When the remaining degree of freedom is less than 6, using this mapping matrix results in an improper solution, given by $\hat{\mathcal{F}}_{EF} = (J_{EF}^T)^\dagger r$.

To address these problems (i.e., unknown joint-locking torques and kinematic degeneracy), two methods for estimating end-effector external wrench based on the F/T sensor at the base are proposed in the following sections: distributed wrench estimation based on recursive Newton-Euler dynamics and centralized wrench estimation based on D'Alembert's principle observer.

[1] However, when pure force is applied, such as in a point contact scenario, estimation is possible with only 3-DOF

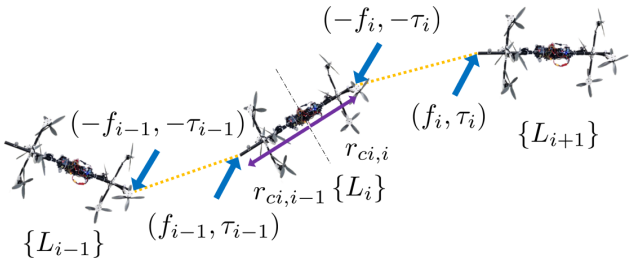

Fig. 3: Internal wrench (f_i, τ_i) between adjacent links $\{L_i\}$ and $\{L_{i+1}\}$, denoted by $i \in 1, 2, \cdots, N$, with a positive direction convention as illustrated. The utilization of joint locking leads to an increase in the internal wrench.

III. Distributed wrench estimation based on recursive Newton-Euler dynamics

A distributed estimation method estimates the external wrench for each link and sequentially calculate the internal wrench at each joint from the base wrench $(\hat{f}_0, \hat{\tau}_0) \in \mathbb{R}^6$ and calculates external wrench at end-effector $(-\hat{f}_n, -\hat{\tau}_n) \in \mathbb{R}^6$. The dynamics of each link of LASDRA are described by

$$\begin{aligned} m_i a_i + m_i g &= u_{m,i} + f_{i-1} - f_i \\ I_i \dot{\omega}_i^b + \omega_i^b \times (I_i \omega_i^b) &= \tau_{m,i}^b + \tau_{i-1}^b - \tau_i^b \\ &+ r_{ci,i-1}^b \times f_{i-1}^b - r_{ci,i}^b \times f_i^b \end{aligned} \tag{5}$$

where $m_i \in \mathbb{R}$, $I_i \in \mathbb{R}^{3\times3}$ are mass and inertia matrix of the i-th link. $R_i \in \mathbb{R}^{3\times3}$ denote the SO(3) orientation of i-th link, respectively. $\omega_i^b \in \mathbb{R}^3$ is the angular velocity of the i-th link expressed in body frame and $g \in \mathbb{R}^3$ is gravitational acceleration vector. $(f_{i-1}, \tau_{i-1}) \in \mathbb{R}^6$ and $(f_i, \tau_i) \in \mathbb{R}^6$ are wrenches applied at proximal side joint and distal side joint of the i-th link, respectively. $r_{ci,i-1} \in \mathbb{R}^3$ and $r_{ci,i} \in \mathbb{R}^3$ are the i-th link center of mass to proximal side joint and distal side joint of the i-th link, respectively, as shown in Fig. 3.

In this method, the external wrench estimation for each link uses MBO on maximal coordinates described by

$$\begin{aligned} r_i^f &= K_i^f[p_i(t) - \int_0^t (u_{m,i} + r_i^f) ds - p_i(0)] \\ r_i^\tau &= K_i^\tau[I_i\omega_i(t) - \int_0^t (\tau_{m,i} - \omega_i \times (I_i\omega_i) + r_i^\tau) ds \\ &\quad - I_i\omega_i(0)] \end{aligned} \tag{6}$$

where $K_i^f, K_i^f \in \mathbb{R}^{3\times3}$ represent observer gain for force and torque estimation, respectively. The observer outputs, r_i^f and r_i^τ, provide the estimated external wrench for the i-th link. After obtaining the external wrench for each link using (6), specify the external wrench due to joint internal wrench by

$$\begin{aligned} f_i^{ext} &= f_{i-1} - f_i + m_i g \\ \tau_i^{ext} &= \tau_{i-1} - \tau_i + r_{ci,i-1} \times f_{i-1} + r_{ci,i} \times (-f_i) \end{aligned} \tag{7}$$

The estimated joint internal wrench $(\hat{f}_i, \hat{\tau}_i) \in se(3)$ can be calculated sequentially from the internal wrench at the previous joint by

$$\begin{gathered}\hat{f}_i = \hat{f}_{i-1} + m_i g - \hat{f}_i^{ext} \\ \hat{\tau}_i = \hat{\tau}_{i-1} + r_{ci,i-1} \times \hat{f}_{i-1} + r_{ci,i} \times (-\hat{f}_i) - \hat{\tau}_i^{ext} \\ \hat{f}_i^{ext} = r_i^f, \ \hat{\tau}_i^{ext} = r_i^\tau \\ \hat{\mathcal{F}}_{EF} := (\hat{f}_{EF}, \hat{\tau}_{EF}) = (-\hat{f}_n, -\hat{\tau}_n)\end{gathered} \tag{8}$$

where, the notation $\hat{\star}$ denotes the estimated value of the $\star$. This wrench propagation algorithm not only provides internal joint torque in the joint rotation axis but also the full 6-DOF internal joint wrench information, irrespective of joint locking. Therefore, This approach overcomes the problem of estimating the internal wrench in LASDRA, which is caused by joint locking, as discussed in Section II-B. To initiate the propagation, the internal wrench at the base $(\hat{f}_0, \hat{\tau}_0)$ needs to be known for estimating the external wrench. To address this, an F/T sensor was installed between the base and the first link. Since external actuation prevents excessive load at the base, the F/T sensor can be safely installed.

The distributed MBO wrench estimation is conceptually simple and can benefit from fast low-level onboard sensors with distributed computation, making it easy to implement for onboard computing. Additionally, if the EAMM has a very long structure, peer-to-peer communication between the links may be necessary. In this case, distributed wrench estimation has the benefit of straightforward implementation from the base to the end-effector.

However, the performance of the distributed MBO heavily relies on the observer gain K_i^f, K_τ^f, and the uncertainty in joint wrench estimation increases as the wrench propagation proceeds from the base during transient estimation processes. Furthermore, it is well-known that distributed algorithms like ours can substantially degrade and even become unstable with a certain combination of observer gain and communication delay/topology (e.g., string stability [15]). This issue can be circumvented by the centralized estimation algorithm to be developed in Sec. IV.

IV. Centralized Wrench Estimation based on D'Alembert's principle

The D'Alembert's principle states that the internal force or torque does not affect the momentum or angular momentum of the entire system, and the work done by the restraining or reaction force on the system is zero. This principle can be extended to torque estimation by considering only the external forces and torques applied to the system. D'Alembert's principle for the 3D rigid body can be written s.t.,

$$\begin{aligned}\sum(\vec{F})_{eff} &= \sum_i m_i a_i \\ \sum(\vec{M}^O)_{eff} &= \sum_i \frac{d}{dt}[\vec{H}_i^G + r_{ci}^{G/O} \times m_i v_i^G]\end{aligned} \tag{9}$$

where $(\vec{F})_{eff}, (\vec{M}^O)_{eff} \in \mathbb{R}^3$ represent the effective force and moment applied to the LASDRA system calculated using kinematics. Frame O is an arbitrary frame, and G is the center of mass of the link. The position vector from frame O to the center of mass of the i-th ODAR is denoted by $r_{ci}^{G/O} = r_{ci} \in \mathbb{R}^3$, and $v_i^G \in \mathbb{R}^3$ represents the linear velocity of the i-th link. The angular momentum $\vec{H}^\star \in \mathbb{R}$ is calculated from frame $\star$. The distributed estimation method described earlier suffers from the drawback of increasing estimation uncertainty due to sequential internal wrench calculations at each joint. This uncertainty can be amplified, especially when EAMM has a long kinematic structure. To overcome this, the D'Alembert's principle can be used to tightly couple the measurement values of the system and improve the estimation.

Using the D'Alembert's principle with the origin set at the junction between the base and the first link, the whole net wrench can be calculated by

$$\begin{aligned}\sum(\vec{F})_{net} &= \sum_i u_{m,i} + \sum_i m_i g + f_{EF} + f_0 \\ \sum(\vec{M}^O)_{net} &= \sum_i \{r_{ci} \times (u_{m,i} + m_i g) + \tau_{m,i}\} \\ &\quad + r_{EF} \times f_{EF} + \tau_{EF} + \tau_0\end{aligned} \tag{10}$$

where $(\vec{F})_{net}, (\vec{M}^O)_{net} \in \mathbb{R}^3$ represent the net force and moment applied to the LASDRA system and $r_{EF} \in \mathbb{R}^3$ is base to end-effector position. This algorithm also requires a base F/T sensor to measure the effective wrench at the base. Direct calculation of the end-effector external wrench using the D'Alembert's principle (9)(10) often leads to noisy output due to the inherent noise in acceleration measurement and F/T sensor output. To address this issue, an observer form is proposed by

$$\begin{aligned}\bar{r}_f &:= \bar{K}_f \int_0^t [\sum(\vec{F})_{eff} - \sum(\vec{F})_{net} + f_{EF} - \bar{r}_f] ds \\ \bar{r}_\tau &:= \bar{K}_\tau \int_0^t [\sum(\vec{M}^O)_{eff} - \sum(\vec{M}^O)_{net} + \tau_{EF} - \bar{r}_\tau] ds\end{aligned} \tag{11}$$

where observer outputs, denoted by $\bar{r}_f \in \mathbb{R}^n$ and $\bar{r}_\tau \in \mathbb{R}^n$, represent the estimated end-effector external force and torque, respectively. The total effective force, $\sum(\vec{F})_{eff}$, is obtained from kinematics (9), while $\sum(\vec{F})_{net}$ is calculated from the total external force (10). Similarly, $\sum(\vec{M}^O)_{eff}$ is obtained from kinematics, while $\sum(\vec{M}^O)_{net}$ is calculated from the total external torque. The observer gain for the estimator based on D'Alembert's principle is represented by $\bar{K}_f \in \mathbb{R}^{3\times3}$ and $\bar{K}_\tau \in \mathbb{R}^{3\times3}$ for force and torque respectively. To calculate (11), the external wrench applied to the end-effector f_{EF} and τ_{EF} are first canceled out, and then the remaining values are integrated. It is important to note that τ_{EF} is calculated after determining f_{EF}, as the latter is required for integration.

In the centralized estimation algorithm, the main computer requires state information of all links, which can lead to potential restrictions in the form factor of the EAMM due

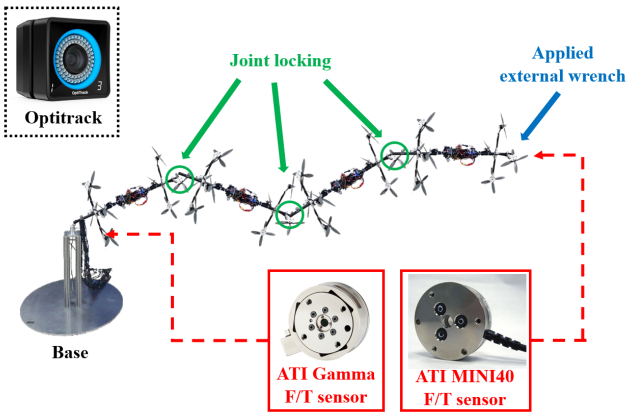

Fig. 4: Experimental setup for external wrench estimation on the 4-Link LASDRA platform. Kinematic information is obtained from Optitrack™ motion capture system, and an ATI-Gamma F/T sensor is installed at the base. An ATI MINI40 F/T sensor is attached to the end-effector to obtain ground truth for external wrenches.

m_i	[1.75, 1.94, 1.92, 1.57] (kg)
I_i	[diag(0.01, 0.1, 0.1), diag(0.01, 0.1, 0.1), diag(0.01, 0.1, 0.1), diag(0.01, 0.1, 0.1)] (kg $*m^2$)
l_i	[1.01, 1.01, 1.01, 1.01] (m)
q_0	[0, 0, 0, 0, 0, 0, 0, 0, 0] (deg)
q^d	[0, 30, 0, 5, 0, -9.5, 0, -0.5, 0] (deg)

TABLE I: Experimental setup and system parameters for 4-Link LASDRA

to wire routing or limitations in communication speed. However, it overcomes the issue of increasing uncertainty in joint wrench estimation observed in the distributed algorithm.

V. Wrench Estimation Performance Validation

A. Experimental Comparison

In the experimental setup, as shown in Fig. 4, we evaluated the performance of the external wrench estimator by utilizing an ATI F/T sensor Gamma attached to the base and an ATI F/T sensor mini 40 attached to the end-effector of 4-Link LASDRA. Since the control box of the ATI F/T sensor is too heavy to attach to LASDRA, and the communication cable of the ATI F/T sensor mini 40 is only about 5m, it was necessary to attach the control box near the base when applying it to the 4-link LASDRA. However, this approach becomes infeasible if the number of LASDRA links is increased due to cable length limitations.

During hovering, LASDRA is applied an external wrench to the end-effector, and we assessed whether the estimator accurately estimated this external wrench. The F/T sensor attached to the end-effector provided true values for comparison but was not used in the estimator. Kinematics information, such as pose and twist, utilized in the estimator, was obtained numerically from Optitrack™ data. The detailed parameters are shown in Table I, where $m_i \in \mathbb{R}^+$, $I_i \in \mathbb{R}^{3\times3}$, and $l_i \in \mathbb{R}^+$ represent the mass, inertia matrix, and length of link i, respectively. The simulation started with an initial configuration $q_0 \in \mathbb{R}^n$, and the LASDRA controller attempted to converge to the desired configuration $q^d \in \mathbb{R}^n$.

Fig. 5 demonstrates that in the case of joint locking, the force estimation using MBO had significant errors, whereas

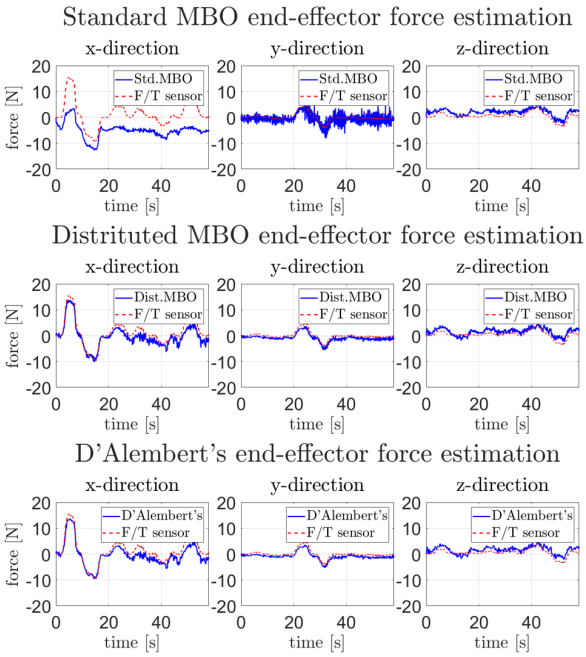

(a) Force estimation result

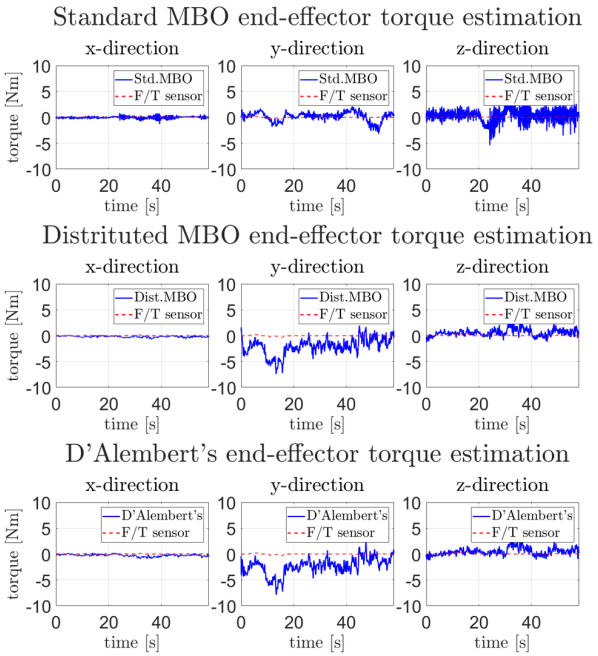

(b) Torque estimation result

Fig. 5: Experimental results of wrench estimation for a 4-link LASDRA using a push-recovery scenario. The standard MBO shows poor estimation performance due to the effect of internal joint locking torque. The distributed estimation algorithm shows no meaningful difference compared to the centralized (D'Alembert's) estimation algorithm, likely because the experiment was conducted with only a few links.

when using the D'Alembert's principle, the force estimator estimated well even when the joints were locked. Although the distributed MBO wrench estimation shows similar results to the D'Alembert-based estimator, this is largely due to the small number of links in the system. The RMSE for the force and torque estimation using MBO, distributed MBO, D'Alembert's principle is shown in Table II.

However, torque estimation in the pitch direction (y-direction) showed larger errors than the standard MBO for both the distributed and centralized algorithms. This discrepancy arises because both methods rely on the base F/T sensor, which reflects the mass parameter error of the link and the thrust error generated by the links. LASDRA, being an EAMM-JL with a very long structure, generates thrust continuously during hovering, resulting in a significant force cancellation in the z-direction. This, in turn, leads to an issue where the torque error in the pitch direction easily increases due to rotor thrust or link's mass parameter errors (e.g., wire mass).

In contrast, the standard MBO does not utilize an F/T sensor at all, which allows it to maintain relatively lower torque estimation errors in the pitch direction, even in the presence of parameter errors. However, the standard MBO shows that the torque estimation errors in the pitch and yaw directions (z-direction) tend to increase simultaneously in the presence of parameter errors.

Force	MBO	Distributed	D'Alembert's
x	6.72 (N)	1.99 (N)	2.07 (N)
y	1.30 (N)	0.95 (N)	1.01 (N)
z	1.59 (N)	1.36 (N)	1.43 (N)

(a) force RMSE

Torque	MBO	Distributed	D'Alembert's
x	0.20 (Nm)	0.35 (Nm)	0.25 (Nm)
y	0.88 (Nm)	2.57 (Nm)	2.86 (Nm)
z	1.21 (Nm)	0.88 (Nm)	0.84 (Nm)

(b) torque RMSE

TABLE II: External wrench estimator RMSE for MBO, distributed MBO, D'Alembert's principle

B. Simulation Comparison

The long structure of LASDRA exacerbates torque estimation errors. To demonstrate the estimation error, a push-recovery simulation was conducted in MATLAB as shown in Fig. 6, using the parameters listed in Table III.

The simulation involves updating the dynamics in generalized coordinates and applying a step external wrench $\mathcal{F}_{EF}$ at the end-effector. The desired joint configuration is set to a constant pitch zig-zag configuration, as shown in Fig. 6. In the absence of signal delay, the distributed MBO force estimation performs well, except for the distributed MBO convergence speed due to MBO gain. However, its torque estimation leads to a noisy outcome due to the transient response of the MBO, causing over/undershoot, as shown in Fig.7.

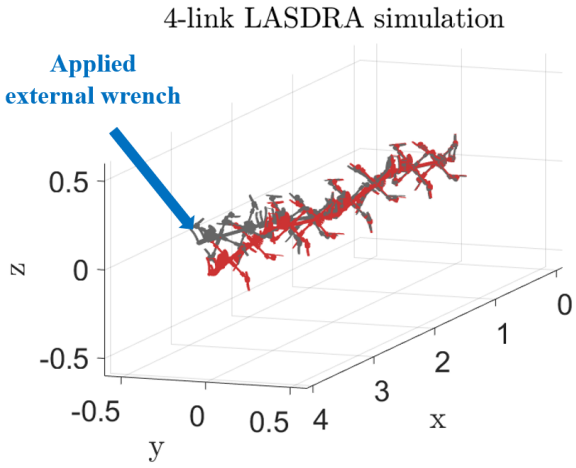

Fig. 6: Simulation of a 4-link LASDRA platform, displaying the current (black) and desired (red) configurations. The LASDRA system is designed to converge toward its desired configuration through distributed impedance control. The simulation was conducted using symplectic Euler integration in generalized coordinates.

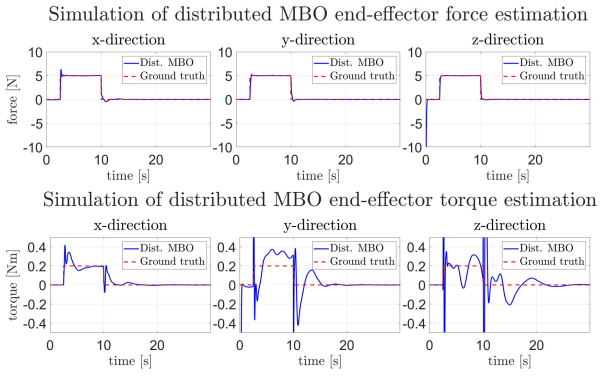

(a) $K_i^f = \text{diag}[20, 20, 20]$, $K_i^\tau = \text{diag}[20, 20, 20]$

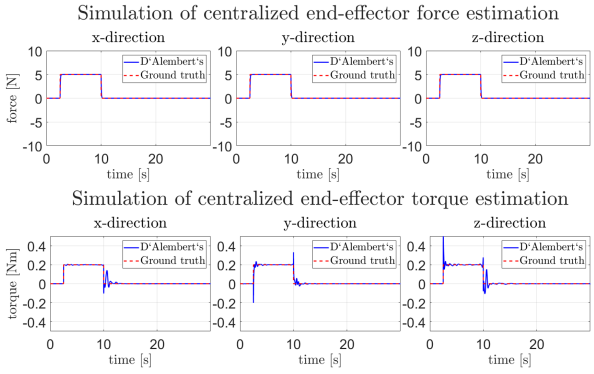

(b) $\bar{K}_f = \text{diag}[20, 20, 20]$, $\bar{K}_\tau = \text{diag}[20, 20, 20]$

Fig. 7: Simulation results of the distributed MBO wrench estimation method demonstrate that the torque estimation exhibits over/undershoot, while the force estimation error remains small. Conversely, the torque estimation of the centralized method shows superior performance compared to the distributed MBO, as it avoids the uncertainty of joint internal wrench estimation.

N	4
Δt	0.005 (s)
m_i	1.5 (kg)
I_i	diag$(0.01, 0.1, 0.1)$ (kg $*m^2$)
l_i	1.01 (m)
$\mathcal{F}_{EF}$	[5, 5, 5] (N), [0.5, 0.5, 0.5] (Nm)
q_0	[0, 0, 0, 0, 0, 0, 0, 0, 0] (deg)
q^d	[0, -5, 0, 10, 0, -10, 0, 10, 0] (deg)

TABLE III: Simulational setup for distributed MBO

The distributed estimation also exhibits substantial accuracy degradation as the number of links increases, due to the interplay between the local MBO dynamics and the delay among them. To verify this, a simulation was conducted where the weight of the link and the applied external wrench remained the same, while the number of links was increased. The results, as shown in Fig. 8, reveal an increase in the torque estimation root-mean-square error (RMSE) between the actual external torque $\tau_{EF} \in \mathbb{R}^3$ and the estimated external torque $\hat{\tau}_{EF} \in \mathbb{R}^3$ with an increase in the number of links. This issue arises due to the convergence characteristics of the observer and wrench propagation. In contrast, the centralized estimation with D'Alembert's principle maintains its performance regardless of the number of links.

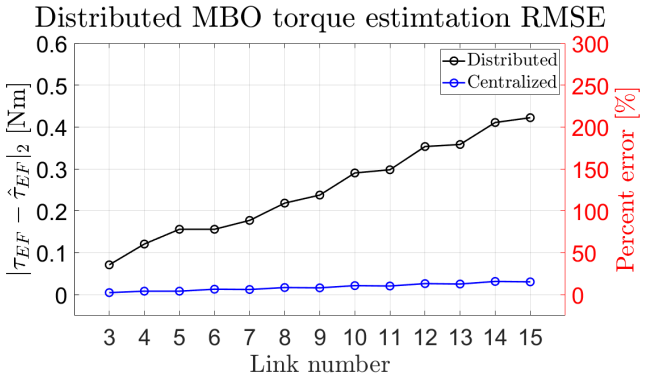

Fig. 8: The 2-norm of RMSE of end-effector torque estimation increases with the number of links N, especially in the distributed estimation. The distributed MBO gain is set to $K_i^f = K_i^\tau = \text{diag}[100, 100, 100]$, while the centralized estimation gain is set to $\bar{K}f = \bar{K}\tau = \text{diag}[100, 100, 100]$. The desired configuration of LASDRA is set to a zig-zag configuration. The percent error is calculated with respect to the applied external wrench, $f_{EF} = [1.0; 1.0; 1.0]$ (N) and $\tau_{EF} = [0.2; 0.2; 0.2]$ (Nm). Signal delays between links are set to be 0.01 (s)

VI. Conclusion

In this paper, we presented two methods for external wrench estimation in the EAMM-JL system: a distributed approach using recursive Newton-Euler dynamics and a centralized approach based on D'Alembert's principle. These methods were designed to overcome the issues of Jacobian-degeneracy and uncertain JL-torques. Through simulations and analysis, we examined the advantages and limitations of both methods. During real flight experiments on the 4-link LASDRA platform with joint locking, both approaches demonstrated superior force estimation compared to the standard MBO algorithm. This finding highlights the effectiveness of our proposed methods in accurately estimating external wrench. In the future, these wrench estimation techniques can be applied to other EAMM-JL platforms, enabling force control in various workspaces and exploring teleoperation possibilities with the wrench estimator.

References

[1] S. Haddadin, A. De Luca and A. Albu-Schäffer, Robot Collisions: A Survey on Detection, Isolation, and Identification. In *IEEE Transactions on Robotics*, vol. 33, no. 6, pp. 1292-1312, 2017.

[2] H. Yang, S. Park, J. Lee, J. Ahn, D. Son, and D. J. Lee. Lasdra: Large-Size Aerial Skeleton System with Distributed Rotor Actuation. In *Proc. IEEE Int'l Conference on Robotics & Automation*, pages 7017–7023, 2018.

[3] H. Lee, Y. Kim, H. Yang, F. Höpflinger and D. Lee. Development of Downsized LASDRA with 2-DoF Joint Locking Device. In *Proc. IEEE Aerial Robotic Systems Physically Interacting with the Environment*, pages 1–4, 2021.

[4] S. Park, Y. Lee, J. Heo and D. J. Lee. Pose and Posture Estimation of Aerial Skeleton Systems for Outdoor Flying. In *Proc. IEEE Int'l Conference on Robotics & Automation*, pages 704-710, 2019.

[5] S. Park, J. Lee, J. Ahn, M. Kim, J. Her, G. Yang, and D. J. Lee. ODAR: Aerial Manipulation Platform Enabling Omnidirectional Wrench Generation. In *IEEE/ASME Transactions on Mechatronics*, 23(4):1907–1918, 2018.

[6] T. Tomić and S. Haddadin, Simultaneous estimation of aerodynamic and contact forces in flying robots: Applications to metric wind estimation and collision detection. In *Proc. IEEE Int'l Conference on Robotics & Automation*, pages 5290–5296, 2015.

[7] F. Shi, M. Zhao, T. Anzai, X. Chen, K. Okada and M. Inaba. External Wrench Estimation for Multilink Aerial Robot by Center of Mass Estimator Based on Distributed IMU System. In *Proc. IEEE Int'l Conference on Robotics & Automation*, pages 1891-1897, 2019.

[8] A. Marino, G. Muscio and F. Pierri, "Distributed cooperative object parameter estimation and manipulation without explicit communication. In *Proc. IEEE Int'l Conference on Robotics & Automation*, pages 2110-2116, 2017.

[9] D. Sanalitro, M. Tognon, A. E. J. Cano, J. Cortés and A. Franchi. Indirect Force Control of a Cable-Suspended Aerial Multi-Robot Manipulator. In *IEEE Robotics and Automation Letters*, 7(3):6726-6733, 2022.

[10] H. Nguyen, S. Park, J. Park and D. J. Lee. A Novel Robotic Platform for Aerial Manipulation Using Quadrotors as Rotating Thrust Generators. In *IEEE Transactions on Robotics*, 34(2):353-369, 2018.

[11] K. Bodie et al. Active Interaction Force Control for Contact-Based Inspection With a Fully Actuated Aerial Vehicle. In *IEEE Transactions on Robotics*, 37(3):709-722, 2021.

[12] M. Ryll et al. 6D Interaction Control with Aerial Robots: The Flying End-Effector Paradigm. In *The Int'l Journal of Robotics Research*, 38(9):1045-1062, 2019.

[13] T. Anzai, M. Zhao, S. Nozawa, F. Shi, K. Okada and M. Inaba. Aerial Grasping Based on Shape Adaptive Transformation by HALO: Horizontal Plane Transformable Aerial Robot with Closed-Loop Multilinks Structure. In *Proc. IEEE Int'l Conference on Robotics & Automation*, pages 6990–6996, 2018.

[14] M. Zhao, T. Anzai, F. Shi, X. Chen, K. Okada and M. Inaba. Design, Modeling, and Control of an Aerial Robot DRAGON: A Dual-Rotor-Embedded Multilink Robot With the Ability of Multi-Degree-of-Freedom Aerial Transformation. In *IEEE Robotics and Automation Letters*, 3(2):1176-1183, 2018.

[15] D. Swaroop and J. K. Hedrick. String stability of interconnected systems. In *IEEE Transactions on Automatic Control*, 41(3):349-357, 1996.